



HAL
open science

Extended germano-gallate fiber drawing domain: from germanates to gallates optical fibers

Théo Guérineau, Clément Strutynski, Téa Skopak, Steeve Morency, Anouar Hanafi, Florian Calzavara, Yannick Ledemi, Sylvain Danto, Thierry Cardinal, Younès Messaddeq, et al.

► To cite this version:

Théo Guérineau, Clément Strutynski, Téa Skopak, Steeve Morency, Anouar Hanafi, et al.. Extended germano-gallate fiber drawing domain: from germanates to gallates optical fibers. *Optical Materials Express*, 2019, 9 (6), pp.2437-2445. 10.1364/OME.9.002437 . hal-02188507

HAL Id: hal-02188507

<https://hal.science/hal-02188507>

Submitted on 18 Jul 2019

HAL is a multi-disciplinary open access archive for the deposit and dissemination of scientific research documents, whether they are published or not. The documents may come from teaching and research institutions in France or abroad, or from public or private research centers.

L'archive ouverte pluridisciplinaire **HAL**, est destinée au dépôt et à la diffusion de documents scientifiques de niveau recherche, publiés ou non, émanant des établissements d'enseignement et de recherche français ou étrangers, des laboratoires publics ou privés.



Extended germano-gallate fiber drawing domain: from germanates to gallates optical fibers

THEO GUÉRINEAU,¹  CLÉMENT STRUTYNSKI,¹ TEA SKOPAK,^{1,2}
STEEVE MORENCY,² ANOUAR HANAFI,² FLORIAN CALZAVARA,¹
YANNICK LEDEMI,² SYLVAIN DANTO,^{1,*} THIERRY CARDINAL,¹
YOUNÈS MESSADDEQ,² AND EVELYNE FARGIN¹

¹Institut de Chimie de la Matière Condensée de Bordeaux (ICMCB), CNRS, UPR 9048, Pessac, 33608, France

²International Associated Laboratory (LIA) LuMAQ: Centre d'Optique, Photonique et Laser (COPL), Université Laval, 2375 rue de la Terrasse, Québec, QC, G1V 0A6, Canada

*sylvain.danto@u-bordeaux.fr

Abstract: Here we report on the production of crystal-free light guiding fibers using a preform-to-fiber approach in the germano-gallate glass system $\text{Ga}_2\text{O}_3\text{-GeO}_2\text{-BaO-La}_2\text{O}_3\text{-Y}_2\text{O}_3$ for various contents of gallium to germanium. For glasses in the system $\text{Ga}_2\text{O}_3\text{-GeO}_2\text{-BaO-K}_2\text{O}$, where surface crystallization precludes fiber drawing from the preform, an open-crucible technique enables the drawing of fiber samples tens of meters long. Cut-back optical attenuation measurements show the extended transmission in the mid-infrared of the produced fibers, up to $2.8\ \mu\text{m}$ with minimum losses of $3.1\ \text{dB/m}$ at $1310\ \text{nm}$ from unpurified glass. These results show that the germano-gallate glasses represent promising mid-infrared materials over an extended fiber drawing domain.

© 2019 Optical Society of America under the terms of the [OSA Open Access Publishing Agreement](#)

1. Introduction

There is currently a critical need in designing new infrared (IR) optical materials for developing integrated IR optical fiber devices, for applications either as passive medium for telecommunication, remote sensing and detection, or as active fiber-laser medium upon doping with luminescent-active elements. Based on their extended transmission in the infrared and their tailorable thermo-mechanical properties, fluoride, tellurite and chalcogenide glasses have been extensively considered as optical components and devices [1]. However, despite their successful technological developments into fibers [2], they still suffer from limitations due to either low transmission in the visible range or relatively poor chemical and mechanical resistance, thus impeding their further effective integration into functional components.

In the meantime heavy metal germano-gallate oxide glasses offer wide optical transparency, extending from $\sim 280\ \text{nm}$ in the UV up to $\sim 6\ \mu\text{m}$ in the mid-IR, high glass transition temperature ($T_g \sim 700\ ^\circ\text{C}$) and superior mechanical strength and laser damage threshold [3,4]. Gallium oxide insertion tends to increase the transmission into the infrared range and the refractive index of the host matrix [5,6]. Wen *et al.* reported on the fabrication of fibers containing up to 19 mol.% of Ga_2O_3 in the Tm^{3+} -doped $\text{BaO-Ga}_2\text{O}_3\text{-GeO}_2$ system [6,7]. Yet, to the best of our knowledge, no optical fiber fabrication has been reported for rich Ga_2O_3 -based glass compositions, a result explained by their larger tendency to crystallization preventing their synthesis and shaping in large amounts.

Recently the authors have explored properties of germano-gallate glasses in the systems $\text{Ga}_2\text{O}_3\text{-GeO}_2\text{-Na}_2\text{O}$ [5], $\text{Ga}_2\text{O}_3\text{-La}_2\text{O}_3\text{-K}_2\text{O}$ [8] and $\text{Ga}_2\text{O}_3\text{-GeO}_2\text{-BaO-K}_2\text{O}$ [9]. Extending this work, we describe here a strategy to manufacture single-index glass fibers of optical quality in the germano-gallate systems $\text{Ga}_2\text{O}_3\text{-GeO}_2\text{-BaO-La}_2\text{O}_3\text{-Y}_2\text{O}_3$ and $\text{Ga}_2\text{O}_3\text{-GeO}_2\text{-BaO-K}_2\text{O}$. First, we

present experimental results obtained by the standard preform-to-fiber method. The introduction of lanthanide oxides La_2O_3 and Y_2O_3 instead of alkali oxide K_2O circumvents the detrimental glass surface crystallization observed previously [9].

In a second approach, we investigate the open-crucible technique for potassium-containing glasses. As it relies on the whole melting of the glass, this method, already largely employed in fluoro-phosphate and chalcogenide glass fiber manufacturing [10,11], eliminates crystallization issues during fiber drawing process. Using this technique, fabrication method for the production of optical fibers in the Ga_2O_3 - GeO_2 - BaO - K_2O glass system is detailed and fiber losses are presented.

2. Experimental details

Glass samples were prepared by the conventional melt-quenching technique from high purity reagents (Ga_2O_3 : 99.998%, Strem Chemical, GeO_2 : 99.999%, Strem Chemical, BaCO_3 : 99%, ACS Merck, K_2CO_3 : 99%, Sigma Aldrich, La_2O_3 : 99.9%, Sigma Aldrich, Y_2O_3 : 99.9%, Alfa Aesar). The powders were mixed in a platinum crucible and heated up to 1500 °C for 2 hours. Glass chunks devoted to drawing experiments by crucible technique were obtained by quenching the melt on a stainless steel plate. Preform-to-fiber drawing experiments require cylindrical glass rods of 40 grams, 10 mm in diameter and approximately 10 cm in length. To that end the glass was melted again and quenched in a stainless steel mold with appropriate sizes, the resulting glass rod being annealed at $T_g - 40$ °C for 4 hours and slowly cooled down to room temperature to remove residual mechanical stress. The thermal drawing ability of the preforms was assessed using dedicated optical fiber drawing towers as further detailed below.

The glass transition (T_g) and onset of crystallization (T_x) temperatures were determined by DSC using a Netzsch Pegasus 404F3 apparatus with glass chunks inserted in a Pt pan at a heating rate of 10 °C/min with a precision of ± 2 °C. The density ρ was measured by immersing a glass chunk in diethyl phthalate at room temperature on a Precisa XT 220A weighing scale (estimated error of ± 0.005 g.cm⁻³). The refractive index was measured by prism coupling on a M-line Metricon 2010/M at 532 nm with an estimated error of ± 0.005 . The optical transmission spectra in the UV-Visible-IR range were obtained from an Agilent Cary 5000 (UV-Visible) and a Bruker spectro-photometers. Powder X-ray diffraction (XRD) was performed on a PANalytical X'pert PRO MPD diffractometer in Bragg-Brentano θ - θ geometry equipped with a secondary monochromator and X'Celerator multi-strip detector. The Cu-K α radiation was generated at 45 kV and 40 mA ($\lambda = 0.15418$ nm). Micro-Raman spectra were recorded in backscattering mode on a confocal micro-Raman spectrometer HR (Horiba/Jobin Yvon) equipped with a Synapse CCD detector. A continuous wave laser operating at 532 nm was used for excitation. Typical resolution used for Raman spectrum acquisition is 2.5 cm⁻¹.

Optical fiber attenuation was recorded using the cut-back method. Measurements were performed in two steps: (i) using a halogen lamp (power of ~ 30 mW measured at the fiber input) as broadband source (350-1700nm) and an optical spectrum analyzer (Ando AQ-6315A OSA) for detection in the Vis-NIR range (400-1600 nm) and (ii) using a fiber supercontinuum source (Le Verre Fluoré, Targazh IRguide, emission range from 0.8 to 4.2 μm), a monochromator (Bruker) and a PbSe detector sensitive in the infrared range (1500-4800 nm). Quality of cleaving was systematically inspected with microscope objective and special attention was paid to limit the fiber curvature during measurement.

3. Results and discussion

First, we investigate the ability of germano-gallate oxide glasses to be drawn from the preform. The investigated glass materials (acronyms, nominal compositions in molar and cationic percent) are summarized in Table 1. Their physicochemical properties are displayed in Table 2. The difference ΔT between the two characteristic temperatures T_g and T_x is most of the time regarded

as a reliable criterion for evaluating the glass thermal stability vs crystallization, in particular for its shaping by thermal process like glass fiber drawing, with targeted values of $\Delta T \geq 100$ -120 °C. In our previous work [9], we identified the glass of composition 28Ga₂O₃-37GeO₂-23BaO-12K₂O (mol.%) (hereafter Ga₂₈Ge₃₇Ba₂₃K) as prone to support preform-to-fiber drawing conditions on the basis of its thermal properties ($T_g = 671$ °C, $\Delta T = 191$ °C). The Ga₂₈Ge₃₇Ba₂₃K glass was further modified by replacing potassium oxide with the rare earth elements lanthanum and yttrium oxides in equimolar ratios, following a work by Wen *et al.* on the fabrication of fiber optics [7]. It is worth noting that in the latter work, GeO₂ content was 65 mol.%, i.e. the main glass constituent. Here the three selected glasses were 28Ga₂O₃-37GeO₂-23BaO-6La₂O₃-6Y₂O₃ (hereafter Ga₂₈Ge₃₇Ba₂₃LaY), 21Ga₂O₃-43GeO₂-24BaO-6La₂O₃-6Y₂O₃ (hereafter Ga₂₁Ge₄₃Ba₂₄LaY) and 15Ga₂O₃-60GeO₂-13BaO-6La₂O₃-6Y₂O₃ (hereafter Ga₁₅Ge₆₀Ba₁₃LaY).

Table 1. Investigated glasses (acronyms, nominal compositions in molar and cationic percent)

Sample	Nominal compositions (mol%)						Nominal compositions (cation mol%)					
	Ga ₂ O ₃	GeO ₂	BaO	K ₂ O	La ₂ O ₃	Y ₂ O ₃	GaO _{3/2}	GeO ₂	BaO	KO _{1/2}	LaO _{3/2}	YO _{3/2}
Ga ₂₈ Ge ₃₇ Ba ₂₃ LaY	28.0	37.0	23.0	-	6.0	6.0	40.0	26.4	16.4	-	8.6	8.6
Ga ₂₁ Ge ₄₃ Ba ₂₄ LaY	21.0	43.0	24.0	-	6.0	6.0	31.7	32.3	18.0	-	9	9
Ga ₁₅ Ge ₆₀ Ba ₁₃ LaY	15.0	60.0	13.0	-	6.0	6.0	23.7	47.3	10.2	-	9.4	9.4
Ga ₂₈ Ge ₃₇ Ba ₂₃ K	28.0	37.0	23.0	12.0	-	-	40.0	26.5	16.5	17.0	-	-

Table 2. Physicochemical properties of the investigated glasses

Sample	T_g (± 2°C)	T_x (± 2°C)	ΔT (± 4°C)	ρ (±0.005 g/cm ³)	n_{532nm} (±0.005)
Ga ₂₈ Ge ₃₇ Ba ₂₃ LaY	735	910	175	5.13	1.780
Ga ₂₁ Ge ₄₃ Ba ₂₄ LaY	728	925	197	5.06	1.805
Ga ₁₅ Ge ₆₀ Ba ₁₃ LaY	736	-	-	4.97	1.796
Ga ₂₈ Ge ₃₇ Ba ₂₃ K	671	832	191	4.34	1.701

The measured characteristic temperatures of the glasses are reported in Table 2. The T_g of the La/Y-containing glasses are ~60 °C higher than the potassium-containing glass, suggesting a significant change of the glass network with the introduction of the rare earth. As compared with the Ga₂₈Ge₃₇Ba₂₃K glass, the stability criterion ΔT of the Ga₂₈Ge₃₇Ba₂₃LaY glass decreases while it remains stable for the Ga₂₁Ge₄₃Ba₂₄LaY glass and even cancels for the germanate Ga₁₅Ge₆₀Ba₁₃LaY glass (no crystallization phenomena detected). The density of the rare earth containing glass ranges from $\rho = 4.97$ g.cm⁻³ up to 5.13 g.cm⁻³, while for the potassium-containing composition the value is 4.34 g.cm⁻³. One can also note a larger refractive index for the rare earth containing glass as compared to the glass Ga₂₈Ge₃₇Ba₂₃K ($\Delta n \sim 0.08$).

Polarized Raman spectroscopy was carried out on the investigated germano-gallate oxide glasses in bulk samples. The polarized vibrational spectrum for each studied glass is shown in Fig. 1.

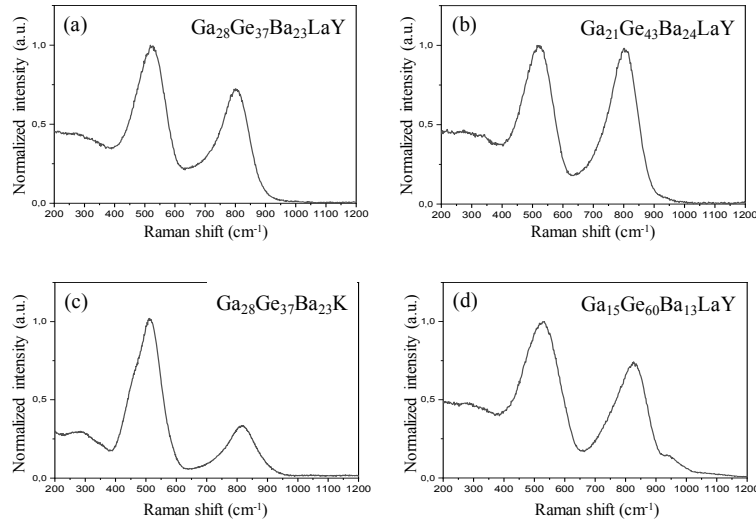


Fig. 1. Raman spectrum of the investigated glasses (a) $\text{Ga}_{28}\text{Ge}_{37}\text{Ba}_{23}\text{LaY}$, (b) $\text{Ga}_{21}\text{Ge}_{43}\text{Ba}_{24}\text{LaY}$, (c) $\text{Ga}_{28}\text{Ge}_{37}\text{Ba}_{23}\text{K}$ and (d) $\text{Ga}_{15}\text{Ge}_{60}\text{Ba}_{13}\text{LaY}$ ($\lambda_{\text{Exc}} = 532 \text{ nm}$)

For all glass compositions, two main contributions can be observed with maximum at around 525 cm^{-1} and 800 cm^{-1} . For the germanate glass (Fig. 1(d)), additional vibrations are observed above 900 cm^{-1} . The band located between 400 cm^{-1} to 600 cm^{-1} is attributed to bending modes involving mainly T–O–T bridges (T used for Ge or Ga in tetrahedral coordination), while the bands between 700 cm^{-1} to 900 cm^{-1} are assigned to localized symmetric and antisymmetric stretching modes of tetrahedral units Ge–O or Ga–O bonds [5]. One can notice for all samples a shoulder at around 760 cm^{-1} .

Previous investigation on sodium germano-gallate glasses [5] has ascribed the bands at 760 cm^{-1} and 860 cm^{-1} to ring structure of germanium and gallium tetrahedral sites in which the sodium ions act as charge compensators. An increase of the sodium concentration, giving rise to a more intense band in relative intensity at around 830 cm^{-1} , was assigned to non-bridging oxygens (NBOs) on the germanium tetrahedral units. Here, for the GeO_2 -rich composition $\text{Ga}_{15}\text{Ge}_{60}\text{Ba}_{13}\text{LaY}$, the band located at 830 cm^{-1} could be attributed to such NBOs with barium or rare earth ions. The spectrum corresponding to the $\text{Ga}_{28}\text{Ge}_{37}\text{Ba}_{23}\text{K}$ (Fig. 1(c)) glass shows also a maximum around 830 cm^{-1} while this vibration is shifted to 805 cm^{-1} for the $\text{Ga}_{28}\text{Ge}_{37}\text{Ba}_{23}\text{LaY}$ and $\text{Ga}_{21}\text{Ge}_{43}\text{Ba}_{24}\text{LaY}$ glasses. Furthermore, the Raman signal of the $\text{Ga}_{28}\text{Ge}_{37}\text{Ba}_{23}\text{LaY}$ and $\text{Ga}_{21}\text{Ge}_{43}\text{Ba}_{24}\text{LaY}$ glasses increases significantly between 620 cm^{-1} and 730 cm^{-1} . Such occurrence appearing for larger amount of gallium oxide could be related to the vibration in this wavenumber range of $[\text{GaO}_4]^-$ and GaO_6 polyhedral units, as suggested in glasses in the Ga_2O_3 - La_2O_3 system or in gallium oxide based garnets [12,13]. At this stage of investigation, one cannot exclude the presence of gallium in octahedral sites as also suggested in the Ga_2O_3 - La_2O_3 glasses.

Then, we conducted drawing experiments on the rare earth containing glass preforms $\text{Ga}_{28}\text{Ge}_{37}\text{Ba}_{23}\text{LaY}$, $\text{Ga}_{21}\text{Ge}_{43}\text{Ba}_{24}\text{LaY}$ and $\text{Ga}_{15}\text{Ge}_{60}\text{Ba}_{13}\text{LaY}$ (Fig. 2). The preforms were drawn using dedicated optical fiber drawing towers, both at the COPL/University Laval and at the ICMCB/University of Bordeaux. The towers are equipped with furnaces having a sharp temperature profile, a diameter and tension controllers, a UV coating unit (optional) and a

collecting drum (Fig. 2). The heating chamber is kept under continuous dry nitrogen gas flow (0.5 L.min⁻¹). Preforms are fed into the furnace and the temperature is gradually increased up to ~940 °C. The bottom-section of the preform is locally softened until forming a drop, which falls down by gravity until being hooked to the collecting drum system (drum velocity: ~4 m.mn⁻¹, preform feed rate: ~1 mm.mn⁻¹). When required, a UV-curable polymer coating (Desolite) was applied on-line during fiber drawing.

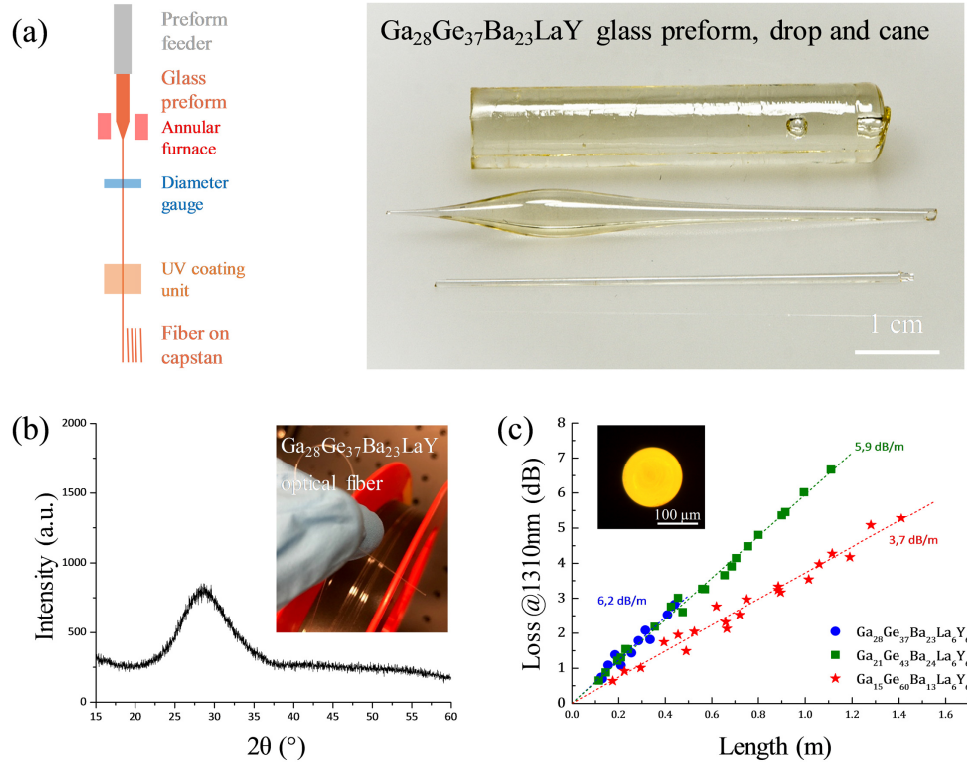


Fig. 2. Preform-based optical fibers manufacturing for GaGeBaLaY glass compositions (a) Scheme of the fiber drawing process and photograph of Ga₂₈Ge₃₇Ba₂₃LaY glass preform, drop and cane (b) XRD pattern of Ga₂₈Ge₃₇Ba₂₃LaY fiber along with a photograph of the fiber on drum, and (c) Loss measurements (inset: fiber cross-sectional view)

Preforms were successfully drawn into tens of meters long fibers with diameters ranging $\phi = 200 \mu\text{m}$, down to $100 \mu\text{m}$. Figure 2(a) depicts a photograph of Ga₂₈Ge₃₇Ba₂₃LaY glass preform prior to drawing, a glass drop and a few centimeters long cane. XRD analyses of the Ga₂₈Ge₃₇Ba₂₃LaY fiber (Fig. 2(b)) shows that the resistance toward devitrification of the selected materials effectively prevents the nucleation and growth of parasitic crystallite centers during the drawing process.

In order to confirm the optical transparency of the fibers, attenuation measurements were performed by the cut-back method at the wavelengths of 1310 nm on initial sections of ~3.0 meters. (Figure 2(c)). We measured optical attenuations of 6.2 dB.m⁻¹, 5.9 dB.m⁻¹ and 3.7 dB.m⁻¹ for the glasses Ga₂₈Ge₃₇Ba₂₃LaY, Ga₂₁Ge₄₃Ba₂₄LaY and Ga₁₅Ge₆₀Ba₁₃LaY respectively.

Experimental results on the Ga₂₈Ge₃₇Ba₂₃K glass are depicted in Fig. 3. The main difficulty to overcome over the process is avoiding crystallization in the softening temperature regime, namely when the glass viscosity is close to 10⁷ Pa.s. While the macroscopic Ga₂₈Ge₃₇Ba₂₃K preform prior to drawing shows no signs of heterogeneities or inclusions (Fig. 3(a)), the preform

neck-down and cane show detrimental surface crystallization preventing the drawing of fibers of optical quality (Fig. 3(b)). This result, which is irrespective of the drawing parameters, is confirmed by XRD analysis of the $\text{Ga}_{28}\text{Ge}_{37}\text{Ba}_{23}\text{K}$ cane (Fig. 3(c)). The XRD pattern presents mixed crystalline peaks indexed by the isostructural phases KGaGeO_4 (JCPDS 052-1595) or BaGa_2O_4 (JCPDS 046-0415).

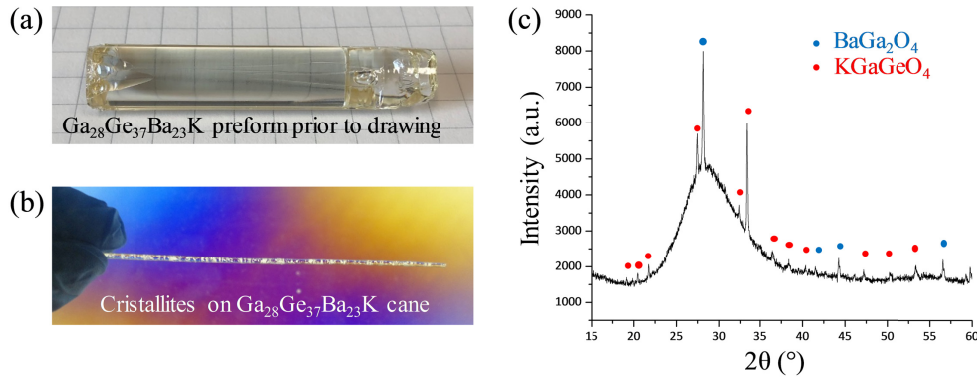


Fig. 3. Preform-based optical fibers manufacturing for $\text{Ga}_{28}\text{Ge}_{37}\text{Ba}_{23}\text{K}$ glass (a) Photograph of macroscopic $\text{Ga}_{28}\text{Ge}_{37}\text{Ba}_{23}\text{K}$ glass preform prior to drawing (b) $\text{Ga}_{28}\text{Ge}_{37}\text{Ba}_{23}\text{K}$ cane and (c) XRD pattern of the $\text{Ga}_{28}\text{Ge}_{37}\text{Ba}_{23}\text{K}$ cane

Surface roughness' at the surface of the $\text{Ga}_{28}\text{Ge}_{37}\text{Ba}_{23}\text{K}$ preforms was considered as a potential issue. Yet, despite polishing treatments to eliminate surface flaws, no noticeable improvement could be achieved. Finally, no loss measurement could be performed on fiber samples drawn from the $\text{Ga}_{28}\text{Ge}_{37}\text{Ba}_{23}\text{K}$ preforms as output signal was undetectable. In fact, the microcrystal formation from the fiber surface produces scattering centers and then parasitic optical losses. This is in good agreement with our previous work [9] showing that the nucleation and growth phenomena in $\text{Ga}_{28}\text{Ge}_{37}\text{Ba}_{23}\text{K}$ glass strongly overlapped and that crystallization of zeolite-type crystalline phases mainly occurs on the surface of the samples as compared to its volume.

The alternative approach explored to produce $\text{Ga}_{28}\text{Ge}_{37}\text{Ba}_{23}\text{K}$ optical glass fibers relies on the open-crucible technique. Here the glass is heated at a much higher temperature than for preform drawing, to reach a sufficiently low viscosity (typically 10^3 - 10^4 Pa.s) to enable the glass flowing through a pinhole located at the bottom of the crucible. Scheme of the method is detailed in Fig. 4(a). After loading in a specifically designed platinum crucible, the $\text{Ga}_{28}\text{Ge}_{37}\text{Ba}_{23}\text{K}$ glass chunks are first heated up to 1200-1300 °C to ensure their complete melting and the absence of any crystallites. Then the temperature is slowly decreased to adjust the glass viscosity until allowing its drawing throughout the hole. Using this method, tens of meters of crystal-free $\text{Ga}_{28}\text{Ge}_{37}\text{Ba}_{23}\text{K}$ glass fiber was obtained with a diameter in the range 180-200 μm (Fig. 4(b)). An acrylic coating was also applied on the fibers during the process. The absorption coefficient spectrum recorded on a $\text{Ga}_{28}\text{Ge}_{37}\text{Ba}_{23}\text{K}$ glass polished slice ($t = 5$ mm) is depicted in Fig. 4(c) (blue line) along with the optical attenuation of the drawn glass fiber (black line). The optical transmission of the bulk $\text{Ga}_{28}\text{Ge}_{37}\text{Ba}_{23}\text{K}$ glass extends from ~ 280 nm to ~ 6.0 μm . The broad absorption near 3.0 μm corresponds to the stretching vibration of free OH^- groups. Loss measurements show that the transmission of the produced fibers extends up to 2.8 μm in the mid-IR, with minimum losses of 3.1 dB/m at 1310 nm. No purification protocol was introduced at this stage, which explains the high loss observed.

In summary, we proposed here two methods for the fabrication of germano-gallate optical fibers. This is to the best of our knowledge the first report on the production of crystal-free, light guiding fibers from a glass composition having gallium oxide as main constituent. While for the

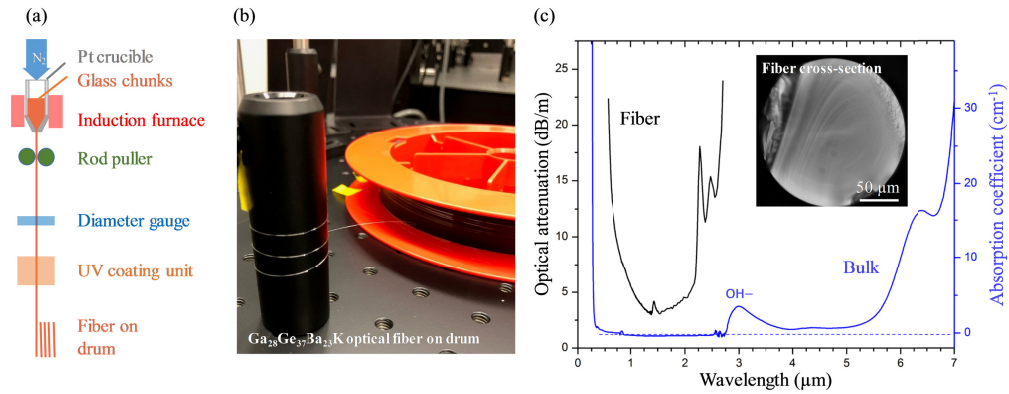


Fig. 4. Open-crucible technique-based optical fiber manufacturing for the $\text{Ga}_{28}\text{Ge}_{37}\text{Ba}_{23}\text{K}$ glass (a) Scheme of the fiber draw process (b) Photograph of the glass fiber on its drum and enrolled on a 25 mm diameter optical post (c) Absorption coefficient spectrum of the $\text{Ga}_{28}\text{Ge}_{37}\text{Ba}_{23}\text{K}$ 5-mm thick bulk glass (blue line) and optical attenuation of the glass fiber drawn by the open-crucible technique. Acrylic coating was removed prior to measurements.

$\text{Ga}_{28}\text{Ge}_{37}\text{Ba}_{23}\text{K}$ glass composition, no fiber could be obtained by preform technology, introduction of lanthanum and yttrium oxides enables to implement preform drawing technology for various content of gallium to germanium. Accordingly to the Raman spectroscopy investigation, the $\text{Ga}_{28}\text{Ge}_{37}\text{Ba}_{23}\text{K}$ glass structure presents a germano-gallate network formed of ring structure of $[\text{GaO}_4]^-$ and GeO_4 , with limited amount of NBOs expected. The introduction of lanthanum and yttrium oxides for the $\text{Ga}_{28}\text{Ge}_{37}\text{Ba}_{23}\text{LaY}$ and $\text{Ga}_{21}\text{Ge}_{43}\text{Ba}_{24}\text{LaY}$ glasses tends to promote the formation of NBOs with the depolymerization of the $[\text{GaO}_4]^-$ and GeO_4 polyhedral based glass network. This structural change is probably at the origin of the disappearance of the surface crystallization of zeolite-type crystalline structures. The relatively high T_g value of the La/Y-containing glasses, as compared to the $\text{Ga}_{28}\text{Ge}_{37}\text{Ba}_{23}\text{K}$ glass composition suggests that the glass structure may be strongly affected by the introduction of the rare earth ions. In the Ga_2O_3 - La_2O_3 glass system [12], Yoshimoto *et al.* have observed that the gallium can occupy tetrahedral and octahedral sites with the presence of NBOs on gallium ions. In GeO_2 - Ga_2O_3 - Na_2O for Ga/Ge ratio around 1, our previous investigation did not evidenced any NBOs on gallium ions using combined NMR and vibrational spectroscopies [5]. One has suggested that ring structure occurs where the alkali ions occupy a compensator role in the structure to balance the charge of the gallium oxide tetrahedra [9].

The preform drawing technique relies on the heating of the glass until attaining its softening at a viscosity close to 10^7 Pa.s. On the other hand, the crucible technique relies on the complete melting of the glass (corresponding to a viscosity of about 10^2 Pa.s), followed by a controlled decrease of temperature and thus of viscosity to attain 10^3 - 10^4 Pa.s, enabling then the fiber drawing throughout the pinhole of the crucible. This technique therefore represents an alternative approach for preventing undesired crystallization to occur during glass drawing, such as for the glass $\text{Ga}_{28}\text{Ge}_{37}\text{Ba}_{23}\text{K}$.

For all the investigated glass compositions, the minimum loss remains relatively high for practical applications. It is important reminding that at this stage, no specific protocols were implemented to purify starting materials and glasses. Works are currently ongoing to improve glass chemical purity, especially to reduce hydroxyl group's content, and to produce core/cladding preforms required for the fabrication of single-mode optical fiber.

4. Conclusion

In this work, we report on the drawing into optical fibers of germano-gallate glasses having various contents of gallium to germanium. We established that lanthanum/yttrium oxides-containing glasses allow the production of crystal-free, light guiding fibers by conventional preform pulling, with optical losses of about 4-6 dB/m at 1310 nm on bare, unpurified fibers. Alternatively, we demonstrated that the crucible technique is a successful approach to suppress the surface crystallization issues faced during the drawing of $\text{Ga}_{28}\text{Ge}_{37}\text{Ba}_{23}\text{K}$ glass preforms, leading to the fabrication of tens of meters-long fiber with minimum losses of 3.1 dB/m at 1310 nm. These results provide insights and practical steps in the shaping into optical fibers of mid-IR vitreous materials having a strong technological potential in optics and photonics.

Funding

Canada Excellence Research Chairs, Government of Canada (CERC); Natural Sciences and Engineering Research Council of Canada (NSERC); Agence Nationale de la Recherche (ANR) (ANR-10-IDEX-03-02, ANR-17-CE08-0042-01).

Acknowledgments

This research was supported by the Canadian Excellence Research Chair program (CERC) in Photonics Innovations and the Aquitaine Region. The authors are also grateful to the Natural Sciences and Engineering Research Council of Canada (NSERC), the Fonds de Recherche Québécois sur la Nature et les Technologies (FRQNT) and the Canadian Foundation for Innovation (CFI) for the financial support. Mobilities were supported by grants of the French Consulate in Québec (by the Frontenac Program), the association of Campus France and Mitacs Globalink as well as grants of the Agence Nationale de la Recherche (ANR) with the program "Investissement d'avenir" number ANR-10-IDEX-03-02 and by the ANR PROTEUS (PRCI ANR-17-CE08-0042-01).

References

1. *The Optical Properties of Optical Glass*, H. Bach and N. Neuroth, eds. (Springer Ed., 1998).
2. G. M. Tao, H. Ebendorff-Heidepriem, A. M. Stolyarov, S. Danto, J. V. Badding, Y. Fink, J. Ballato, and A. F. Abouraddy, "Infrared fibers," *Adv. Opt. Photonics* **7**(2), 379–458 (2015).
3. P. L. Higby and I. D. Aggarwal, "Properties of barium gallium germanate glasses," *J. Non-Cryst. Solids* **163**(3), 303–308 (1993).
4. S. S. Bayya, B. B. Harbison, J. S. Sanghera, and I. D. Aggarwal, "BaO-Ga₂O₃-GeO₂ glasses with enhanced properties," *J. Non-Cryst. Solids* **212**(2-3), 198–207 (1997).
5. T. Skopak, S. Kroeker, K. Levin, M. Dussauze, R. Méreau, Y. Ledemi, T. Cardinal, E. Fargin, and Y. Messaddeq, "Structure and properties of gallium-rich sodium germano-gale glasses," *J. Phys. Chem. C* **123**(2), 1370–1378 (2019).
6. X. Wen, G. W. Tang, Q. Yang, X. D. Chen, Q. Qian, Q. Y. Zhang, and Z. M. Yang, "Highly Tm³⁺ doped germanate glass and its single mode fiber for 2.0 μm laser," *Sci. Rep.* **6**(1), 20344 (2016).
7. X. Wen, G. W. Tang, J. W. Wang, X. D. Chen, Q. Qian, and Z. M. Yang, "Tm³⁺ doped barium gallo-germanate glass single-mode fibers for 2.0 μm laser," *Opt. Express* **23**(6), 7722–7731 (2015).
8. T. Skopak, B. Serment, Y. Ledemi, M. Dussauze, T. Cardinal, E. Fargin, and Y. Messaddeq, "Structure-properties relationship study in niobium oxide containing GaO_{3/2}-LaO_{3/2}-KO_{1/2} gallate glasses," *Mater. Res. Bull.* **112**, 124–131 (2019).
9. T. Skopak, F. Calzavara, Y. Ledemi, F. Célarié, M. Allix, E. Véron, M. Dussauze, T. Cardinal, E. Fargin, and Y. Messaddeq, "Properties, structure and crystallization study of germano-gallate glasses in the Ga₂O₃-GeO₂-BaO-K₂O system," *J. Non-Cryst. Solids* **514**, 98–107 (2019).
10. G. Galleani, Y. Ledemi, E. S. de Lima, S. Morency, G. Delaizir, S. Chenu, J. R. Duclere, and Y. Messaddeq, "UV-transmitting step-index fluorophosphate glass fiber fabricated by the crucible technique," *Opt. Mater.* **64**, 524–532 (2017).
11. J. Lapointe, Y. Ledemi, S. Loranger, V. L. Iezzi, E. S. de Lima, F. Parent, S. Morency, Y. Messaddeq, and R. Kashyap, "Fabrication of ultrafast laser written low-loss waveguides in flexible As₂S₃ chalcogenide glass tape," *Opt. Lett.* **41**(2), 203–206 (2016).

12. K. Yoshimoto, A. Masuno, M. Ueda, H. Inoue, H. Yamamoto, and T. Kawashima, "Low phonon energies and wideband optical windows of La_2O_3 - Ga_2O_3 glasses prepared using an aerodynamic levitation technique," *Sci. Rep.* **7**(1), 45600 (2017).
13. V. Monteseuro, P. Rodríguez-Hernández, R. Vilaplana, F. J. Manjón, V. Venkatramu, D. Errandonea, V. Lavín, and A. Muñoz, "Lattice dynamics study of nanocrystalline yttrium gallium garnet at high pressure," *J. Phys. Chem. C* **118**(24), 13177–13185 (2014).